L-erythrulose synthesis from glycerol by a multi-enzymatic cascade reaction

Aurélien Doutry,[1] Cédric Gastaldi,[1]Maela Claeys,[1] Jean-Louis Petit,[3] Véronique de Berardinis,[3] Christine Guérard-Hélaine,[2] Damien P. Debecker[1]**

[1] Institute of Condensed Matter and Nanosciences (IMCN), Université catholique de Louvain (UCLouvain), 1348 Louvain-la-Neuve, Belgium
[2]Université Clermont Auvergne, Clermont Auvergne INP, CNRS, Institut de Chimie de Clermont-Ferrand, 63000 Clermont-Ferrand, France
[3]Génomique Métabolique, Genoscope, Institut François Jacob, CEA, CNRS, Univ-Evry, Université Paris-Saclay, Evry-Courcouronnes, 91057 Evry, France

* christine.helaine@uca.fr
* damien.debecker@uclouvain.be

Abstract

Upgrading glycerol, an abundant bio-based platform chemical, into high-value oxygenates is a cornerstone of integrated biorefineries. While chemo-catalytic routes typically lack selectivity, enzymatic approaches are often limited in productivity and robustness. Glycerol dehydrogenase (GDH) catalyzes the selective oxidation of glycerol, into the valuable compound dihydroxyacetone (DHA). However, this biocatalytic reaction is hampered by strong product inhibition of the enzyme and by the requirement for the costly cofactor NAD^+. The enzyme is also inhibited by the formed NADH. To overcome these limitations, we designed a biocatalytic cascade system. In this approach, fructose-6-phosphate aldolase (FSA_{A129S}) rapidly converts DHA, thereby preventing inhibition and funneling the reaction toward the formation of L-erythrulose, a stable, non-inhibitory, and more valuable product. In addition, an optimized cofactor regeneration system based on NADH oxidase and catalase is incorporated, so that only a catalytic amount of NAD^+ is required. All four enzymes are co-immobilized on a resin to create a multifunctional heterogeneous biocatalyst. Using this system, L-erythrulose is produced at concentrations up to 120 mM with complete selectivity.

1. Introduction

In recent years, the chemical industry has increasingly shifted from petroleum-based raw materials to biomass-derived resources, aiming for a more sustainable and long-term approach. Among the numerous bio-based molecules available in large quantities from biorefineries, glycerol (1,2,3-propane triol) stands out as a crucial bio-based platform chemical [1,2]. Currently, glycerol is cheaply available as a byproduct of biodiesel production through oil transesterification [3,4]. This versatile molecule is renewable, non-toxic, biodegradable, inexpensive, edible, and highly functionalized, making it amenable to further upgrading. It can be converted into numerous valuable chemicals such as polymers [5,6], ethers [7,8], carbonates [9–11], and various fine chemicals, which are valuable for the cosmetics, pharmaceuticals, chemicals, and food industries [12].

Glycerol oxidation is one of the most interesting valorization pathways, leading to valuable chemicals such as glyceraldehyde or dihydroxyacetone (DHA). DHA finds numerous applications in the chemical industry [13]. The production of DHA from glycerol oxidation can be achieved through chemo-catalytic methods, using noble metal based catalyst (Au, Ag, Pd and Pt) and molecular oxygen as the oxidant [14–17]. However, in such oxidation processes, side products are classically formed via overoxidation reactions [17] so that activity inevitable comes at the expense of selectivity. This makes DHA a difficult target for chemo-catalysis.

The utilization of enzymes for this type of reaction is particularly advantageous owing to their intrinsically high selectivity. Glycerol dehydrogenase (GDH) is known to efficiently catalyze the oxidation of glycerol to DHA [18]. Like many oxidoreductases, this enzyme requires a nicotinamide cofactor (i.e. $NAD(P)^+$) to operate. Noteworthily, GDH is inhibited by the formed NADH, meaning that NAD^+ cannot be added in large excess or even in stoichiometric quantities (which anyway would not be economically viable) and instead must be used in catalytic

amounts and continuously recycled. Various cofactor regeneration systems have been reported in the literature [19,20]. NADPH oxidase (NOX) is a well-documented enzyme, which has already been exploited in combination with GDH [21–23]. During the regeneration of NAD^+ by NOX, H_2O_2 is produced. To prevent potential oxidative damage and side reactions caused by H_2O_2, catalase is classically added to the system. Catalase swiftly catalyzes the decomposition of H_2O_2 into H_2O and O_2, thereby preventing enzyme degradation [24]. However, GDH encounters another crucial limitation: inhibition by its own product, DHA. It is reported that GDH loses 50% of activity in the presence of only 0.42 mM DHA [18]. With these constraints, GDH is arguably underexploited, and the few reports on the GDH-catalyzed oxidation of glycerol show final concentrations of DHA never exceeding the millimolar range (~9 mM at best) [21,22,25].

Here, we propose to further convert DHA (132 $/kg [17]) into an even more valuable product that does not inhibit GDH: L-erythrulose (Figure 1). This ketose is classified as a “rare sugar” and has a high market value (262$/kg BIOSYNTH®). It is primarily used as a tanning agent in the cosmetics industry due to its reactivity with amino acids in the upper skin layers [26]. Additionally, it serves as a source of chiral ethyl ketones in aldol reaction organic synthesis (e.g. in the synthesis of thioesters [27] or polyether antibiotics [28]). The alpha carbonyl group serves as a key site for the attachment of additional carbon fragments through nucleophilic addition [29]. L-erythrulose can be effectively synthesized through the aldolization of formaldehyde and DHA through a biocatalytic route using the D-fructose-6-phosphate aldolase (FSA_{A129S}) [30]. The FSA_{A129S} mutant from *Escherichia coli* has been reported as highly active and robust, making it a suitable catalyst for this organic synthesis cascade [31].

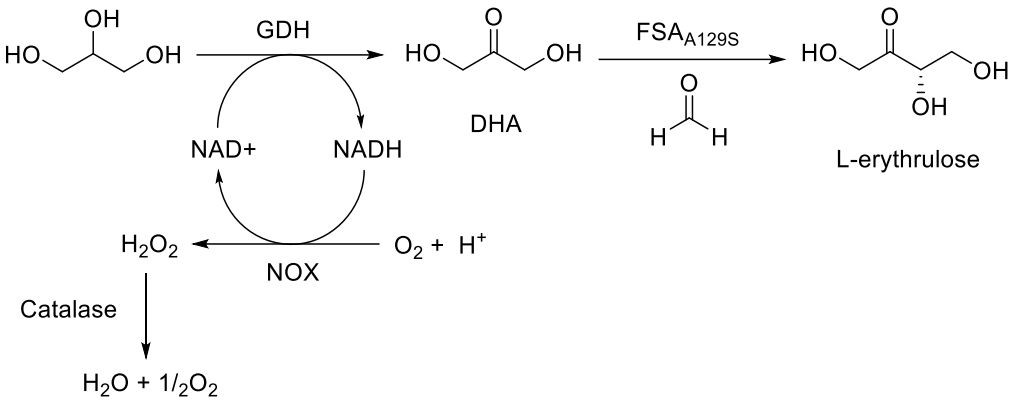

Figure 1: *Multi enzymatic cascade reaction for the enantioselective synthesis of L-erythrulose from glycerol, using a GDH/FSA$_{A129S}$/NOX/Catalase system.*

It should be noted that several reports showed enzymatic cascade reactions aiming at the valorization of glycerol into rare sugars [32–36]. However, to the best of our knowledge, these cascades necessarily involve a phosphorylation step and the use of dihydroxyacetone phosphate (DHAP) aldolase, which increases the overall number of steps and complicates the process. In contrast, our objective is to employ well-characterized and easily producible enzymes to directly synthesize the rare sugar L-erythrulose without requiring phosphorylation, and in a one-pot concurrent cascade reaction.

Here, in the process of glycerol upgrading, the incorporation of FSA$_{A129S}$ "kills two birds with one stone": (i) it provides direct access to a more valuable end-product than DHA and (ii) it mitigates the GDH inhibition. Moving further in the direction of a sustainable chemical synthesis process [37], we also show that the reaction can pushed to high L-erythrulose titer and can be catalyzed in a heterogenous fashion, by using immobilized enzymes.

2. Results and Discussion

2.1 L-erythrulose synthesis by a multi-enzyme cascade reaction (GDH/FSA$_{A129S}$/NOX/Catalase)

The complete cascade reaction was tested starting from 50 mM glycerol, 50 mM formaldehyde, 0.5 mM NAD^+, 0.5 mM NADH in PPi buffer pH 9 at 25°C (Table 1, entry a). The reaction was carried out at pH 9 because NOX and FSA$_{A129S}$ operate optimally under slightly alkaline conditions (8-8.5) [31,38]. Catalase remains highly active over a broad pH range (4–10) [39], while GDH exhibits optimal activity around pH 9 [40]. Since GDH is the rate-limiting enzyme in the system, the reaction pH was set to favor its activity. Under these conditions, 24% glycerol is converted with 100% selectivity, yielding a final L-erythrulose concentration of 12 mM (which is higher than the reported final concentration of DHA for the GDH-catalyzed oxidation of GLY [21,22,25]). The progress of the reaction was monitored by proton NMR, as is commonly reported in the literature [41–43]. No DHA was detected (see ESI, Figure S8), which is consistent with the fact that FSA$_{A129S}$ is very active and drives the rapid conversion of this intermediate towards the final product.

To demonstrate the importance of each enzyme in the system, we repeated this experiment by removing one enzyme at a time (Table 1b, c, d and e). As expected, in the absence of GDH (entry b), no consumption of glycerol was observed and, consequently, no production of L-erythrulose. When NOX was missing (entry c), only a small production of L-erythrulose was noticed, which exactly corresponds to the initial amount of NAD^+ in the solution (0.5 mM). This shows that the cofactor regeneration enzyme is essential. In the absence of FSA$_{A129S}$ (entry d) no L-erythrulose was produced and the conversion of glycerol was markedly reduced as compared to the complete cascade (entry a). This confirms a strong inhibition of GDH by DHA, as described in the literature [18]. Finally, without catalase (entry e), the production of L-erythrulose decreased by 50% in comparison with the standard test (entry a), demonstrating the

importance of this enzyme to rapidly decompose H_2O_2 and avoid its deleterious effects on the other enzymes at work [44].

Introducing NAD^+ only (instead of an equimolar concentration of NAD^+ and NADH) had only a minor effect on glycerol conversion (entry f). Increasing the NAD^+ concentration to 1 mM and 1.5 mM (entries g and h) resulted in a decrease in final L-erythrulose concentration. This effect is most likely caused by the inhibition of an enzyme within the cascade by NAD^+.

In attempts to boost the final L-erythrulose concentration, enzyme loadings were systematically varied. As anticipated, a lower concentration of GDH (0.25 mg/mL, entry i) correlated with a reduced glycerol conversion. However, at 2 mg/mL (entry j), no further increment in production was observed as compared to the starting conditions (1 mg/mL, entry a), hinting to a kinetic bottleneck elsewhere in the enzymatic cascade. In contrast, increasing the concentration of NOX (entry k) resulted in a product yield that surpassed that of the standard conditions (entry a). Thus, the standard conditions revealed a deficiency in NADH recycling which elucidates the absence of enhancement when GDH concentrations were escalated. A further increase in NOX loading from 1.5 mg/mL to 2.25 mg/mL (entry l) did not yield a corresponding rise in L-erythrulose production, suggesting that beyond 1.5 mg/mL, NAD^+ consumption by GDH becomes limiting. Reducing the FSA_{A129S} loading from 5 mg/mL to 1 mg/mL decreased the final L-erythrulose concentration only marginally (entry m), in good agreement with the high efficiency of this enzyme [30]. Notwithstanding, to prevent any possible inhibition of GDH by DHA by ensuring a fast consumption of the intermediate, a concentration of 5 mg of FSA_{A129S} was retained for subsequent assays. Doubling the amount of catalase revealed no significant change in the results (entry n), which aligns with expectations given the high activity of this enzyme (30,000 U/mg); further increase in catalase concentration is deemed unnecessary. Ultimately, building on prior findings, both GDH and NOX concentrations were elevated concurrently (entry o), leading to a notable 19 mM L-erythrulose production.

Table 1: *Glycerol conversion and L-erythrulose concentrations synthesized by the multi-enzymatic cascade as a function of reaction conditions. Reactions conditions: 25°C, 100 mM PPi at pH 9, after 24h, 50 mM glycerol, 50 mM formaldehyde.*

Entry	GDH [mg/mL]	NOX [mg/mL]	FSA_{A129S} [mg/mL]	Catalase [mg/mL]	NAD^+ [mM]	NADH [mM]	Glycerol conversion [%][b]	L-erythrulose concentration [mM][b]
(a)[a]	1	0.75	5	1	0.5	0.5	24	12
(b)	0	0.75	5	1	0.5	0.5	0	0
(c)	1	0	5	1	0.5	0.5	1	0.5
(d)	1	0.75	0	1	0.5	0.5	2	0
(e)	1	0.75	5	0	0.5	0.5	12	6
(f)	1	0.75	5	1	0.5	0	19	9.5
(g)	1	0.75	5	1	1	0	15	7.5
(h)	1	0.75	5	1	1.5	0	0	0
(i)	0.25	0.75	5	1	0.5	0	18	9.5
(j)	2	0.75	5	1	0.5	0	26	13
(k)	1	1.5	5	1	0.5	0	29	14
(l)	1	2.25	5	1	0.5	0	30	15
(m)	1	0.75	1	1	0.5	0	19	9.5
(n)	1	0.75	5	2	0.5	0	24	12
(o)[a]	2	1.5	5	1	0.5	0	38	19

[a] Experiments performed in triplicate to test repeatability. Entry (a) gave a glycerol conversion of 24 ± 1.5 % and a final L-erythrulose concentration of 12 ± 0.7 mM. Entry (o) gave a glycerol conversion of 38 ± 1.2 % and a final L-erythrulose concentration of 19.3 ± 0.6 mM.
[b] Quantified by NMR

To better characterize the enzymatic cascade, inhibition assays were conducted on individual enzymes (see ESI, Section 6). The inhibition of GDH by DHA is well-documented [18]. L-erythrulose did not provoke GDH deactivation (Table S4). On the contrary, inhibition tests with formaldehyde (Table S2) showed GDH was progressively deactivated when increasing the aldehyde concentration. However, incubating the enzyme for 3 h with formaldehyde and then testing it in the regular reaction conditions led to complete deactivation (Table S2). Deactivation by formaldehyde is a well-known phenomenon affecting many enzymes [34]. However, FSA_{A129S} was previously shown to tolerate formaldehyde concentrations exceeding 100 mM [45]. NOX was found to be deactivated by formaldehyde (whether simply added during reaction or incubated for 3 h prior reaction) (Table S1). Inhibition tests with DHA also showed significant NOX inactivation (Table S3), further supporting the relevance of cascading GDH

with FSA_{A129S} to ensure rapid conversion of this intermediate. L-erythrulose concentration did not affect NOX activity (Table S4).

Considering the significant inhibitory effect of formaldehyde, a fed-batch strategy was imagined for the addition of formaldehyde to enhance the L-erythrulose yield. The cascade reaction was performed with a lower initial concentration of formaldehyde (10 mM). After 1, 2, 4, and 6 h, 0.75 µL of formaldehyde (10mM) were added to the solution. The resulting kinetics are shown in Figure 2. The L-erythrulose yield for the "Free enzymes with fed-batch" approach was higher at every time point, reaching 23 mM of L-erythrulose after 24h, which represents an increase of nearly 20%.

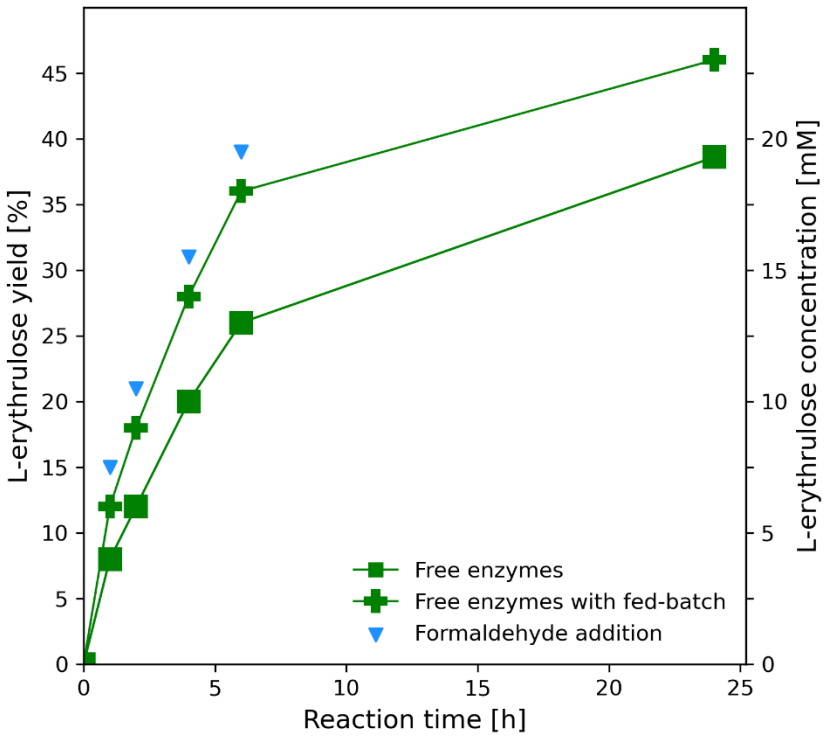

Figure 2: *Evolution of L-erythrulose yield and concentration as the function of reaction time. Blue arrows illustrate the additions of formaldehyde (10 mM each). Initial reactions conditions: 25°C, 100 mM PPi pH 9, 50 mM glycerol, 50 mM formaldehyde or 0.75 µL (10 mM) for the fed-batch, 0.5 mM NAD^+, 2 mg/mL GDH, 1.5 mg/mL NOX, 5 mg/mL FSA_{A129S} and 1 mg/mL catalase.*

2.2 L-erythrulose synthesis by an immobilized multi-enzyme cascade reaction (GDH/FSA$_{A129S}$/NOX/Catalase)

Enzyme immobilization is the go-to strategy in the perspective of industrial application, as it facilitates enzyme recycling and reuse, and is known to often enhance enzyme stability and robustness [46–48]. Here, a commercial support, Relizyme^{TM} enzyme carriers HFA112/S, functionalized with amino-epoxy groups [49–52], was utilized. The enzymes were put in solution in concentrations that correspond to the optimum identified earlier with free enzymes (2 mg/mL GDH, 1.5 mg/mL NOX, 5 mg/mL FSA$_{A129S}$, and 1 mg/mL catalase) and then mixed with the resin for 16 h at 25°C. The resin was subsequently separated by sedimentation and is denoted "Co-immobilized enzymes" (see ESI, Section 8). A Bradford assay was performed on the remaining solution to estimate the enzymes loading. No proteins were detected, demonstrating quantitative immobilization of the four enzymes. The kinetics of the cascade reaction catalyzed by the co-immobilized enzymes is shown in Figure 3. The four enzymes were also immobilized separately, and a cascade reaction was run by adding the four solids, keeping the same overall enzyme loading and ratios (see "Separated immobilized enzymes" in Figure 3). The co-immobilized enzymes exhibited a higher yield at all time points, probably hinting to a beneficial proximity effect between the enzymes. However, after 24 hours, the L-erythrulose yields of both systems became comparable. Enzyme immobilization also appeared to contribute to protecting the enzymes against formaldehyde inhibition, since the final yield obtained in this case (48%) was higher than with the free enzymes (38%), when using 50 mM initial formaldehyde concentration.

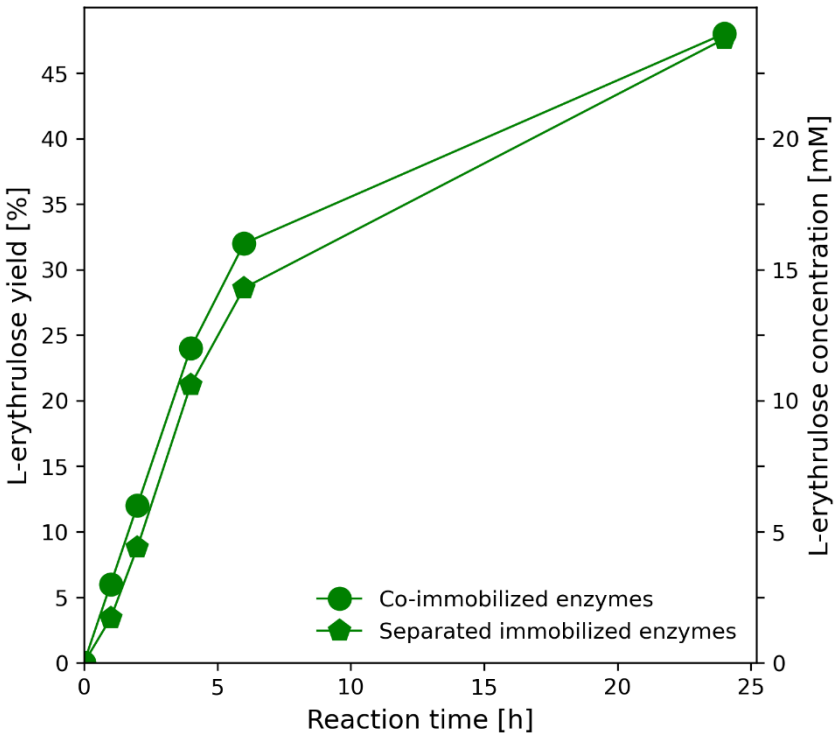

Figure 3: *Evolution of L-erythrulose yield and concentration as the function of reaction time. Initial reactions conditions: 25°C, 100 mM PPi pH 9, 50 mM glycerol, 50 mM formaldehyde, 0.5 mM NAD^+, 2 mg/mL GDH, 1.5 mg/mL NOX, 5 mg/mL FSA_{A129S} and 1 mg/mL catalase.*

In a separate experiment (Figure 4, "Immobilized enzyme with hot filtration test"), the resin with co-immobilized enzymes was removed from the reaction medium after 6 hours. At this point, the L-erythrulose yield had reached 30%; this concentration did not increase further after 24 hours, confirming that the enzymatic activity was solely associated with the solid phase. Furthermore, a Bradford assay performed on the liquid reaction medium verified the absence of enzyme leaching; no protein was detected. Together, these two tests confirmed the effective heterogenization of the catalyst without enzyme leaching.

As with the free enzymes, fed-batch addition of formaldehyde increased the overall yield obtained with the co-immobilized enzymes (Figure 4, "Immobilized enzymes with fed-batch"). Both the activity and the final sugar yield (59%) increased owing to the lower formaldehyde concentration in the medium, which helped prevent enzymes deactivation.

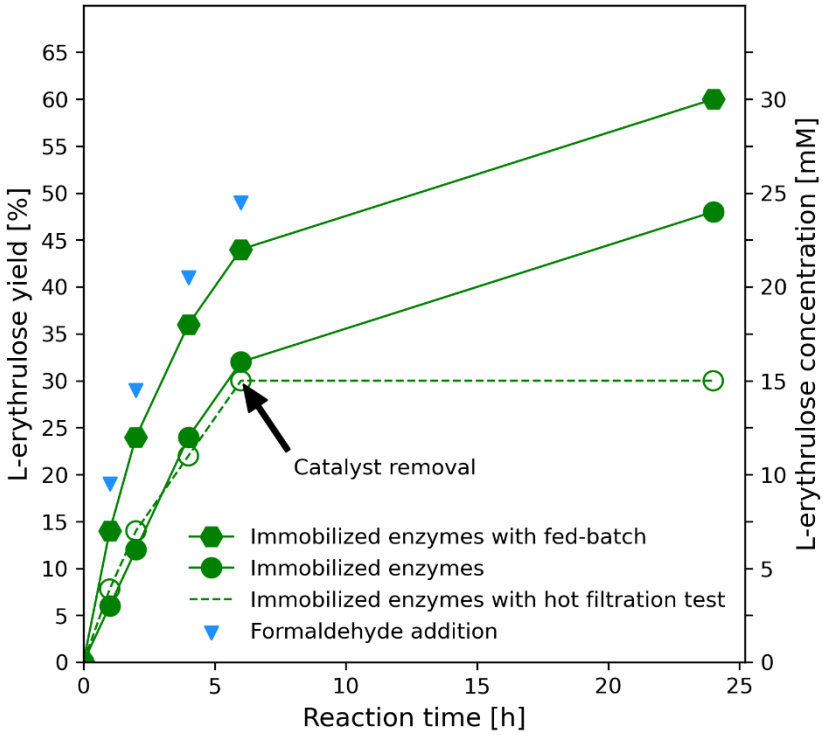

Figure 4: *Evolution of L-erythrulose yield and concentration as the function of reaction time. Reactions conditions: 25°C, 100 mM PPi pH 9, 50 mM glycerol, 50 mM formaldehyde (except for the experiment labelled "Immobilized enzymes with fed-batch, where the initial formaldehyde concentration was 10 mM and the blue arrows indicate further additions of 0.75 µL representing 10 mM of formaldehyde), 0.5 mM NAD^+, 2 mg/mL GDH, 1.5 mg/mL NOX, 5 mg/mL FSA_{A129S} and 1 mg/mL catalase.*

However, extending the reaction time to 5 days resulted in only a marginal increase in the final L-erythrulose yield: the system appears constrained to a maximum yield of approximately 50%. To investigate this, the initial activity of each individual enzyme (GDH, NOX, and FSA_{A129S}) was tested in dedicated enzymatic assays (see ESI Section 2) and the same assays were done after 24h incubation in respective reaction media (Figure 5). These tests were not done for catalase considering its high activity. At t_0, the immobilized GDH, NOX and FSA_{A129S} all exhibited slightly higher specific activities than their free counterparts. After 24 h in the reaction media, the activity of FSA_{A129S} and GDH was slightly decreased for the free enzymes but remained relatively stable for the immobilized enzymes, highlighting the improved operational stability conferred by immobilization. In contrast, NOX activity dropped to nearly undetectable levels after 24 h for both free and immobilized forms. This result confirms NOX deactivation

in operating conditions as the culprit for the apparent limit in L-erythrulose yield; it is indeed well-established, that this enzyme NOX is prone to deactivation by oxygen [53,54].

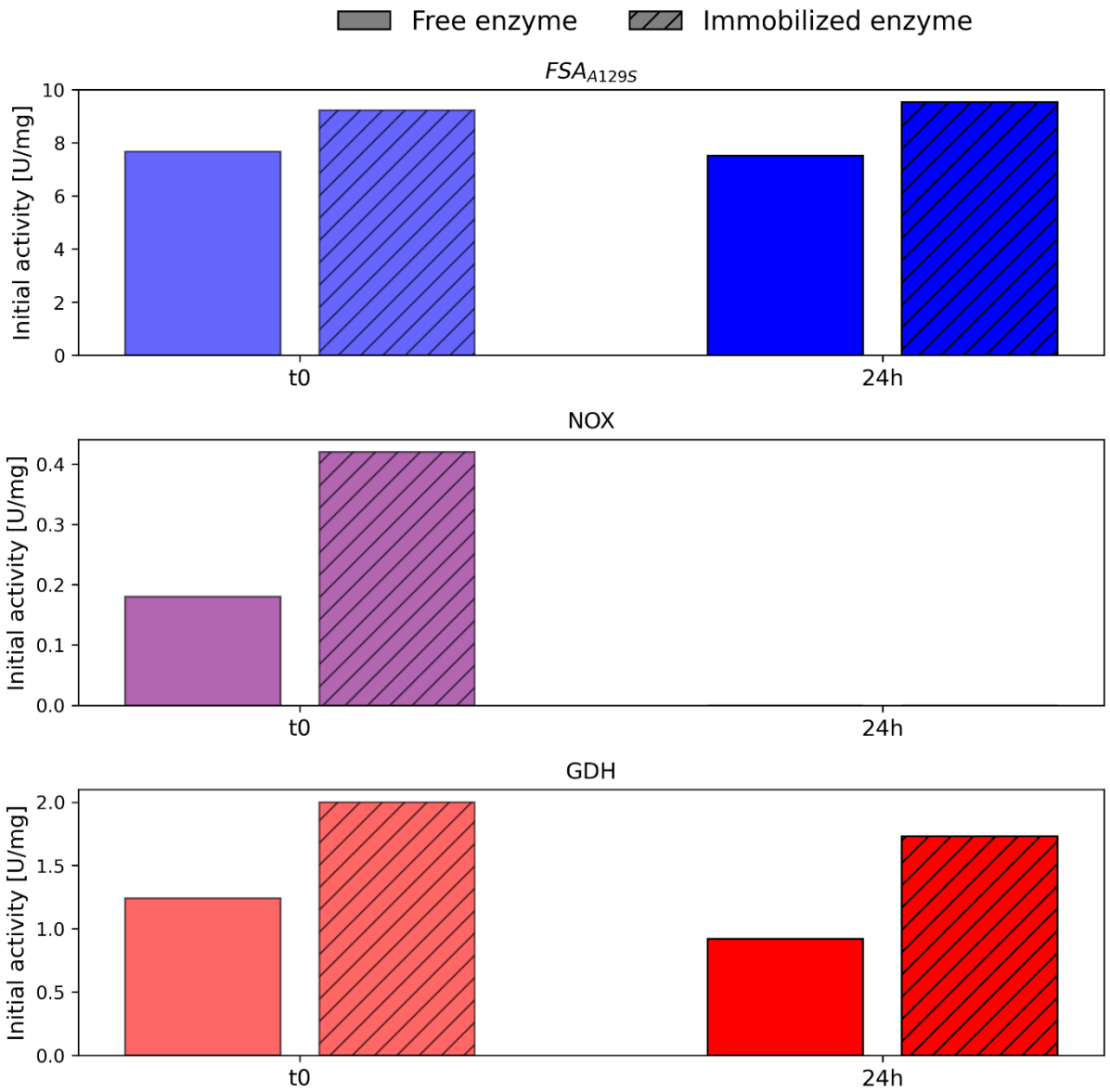

Figure 5: *Enzymatic activity of free and immobilized enzymes at the initial time (t_0) and after 24 h in solution. Activities of FSA$_{A129S}$, NOX, and GDH were measured and expressed as U/mg.*

To complete the study, recyclability tests were carried out. In the first case, the resin containing the four co-immobilized enzymes was used for a 1-hour test, and then the resin was recovered, washed with PPi buffer, and directly reused. This procedure was repeated five times, and the results are presented in Figure 6 (left). The L-erythrulose yield decreased progressively with

each cycle. In contrast, when only GDH, FSA_{A129S}, and catalase were co-immobilized while fresh free NOX was supplied at each cycle in Figure 6 (right), the L-erythrulose concentration remained constant. These results confirm that NOX deactivation is the key limiting factor in the process. With this knowledge, the cascade reaction with the co-immobilized enzyme was repeated but this time, fresh NOX was added to the reaction medium after 24h. This addition led to the resumption of L-erythrulose production, reaching 35 mM after 48 h, corresponding to a glycerol conversion of 70%.

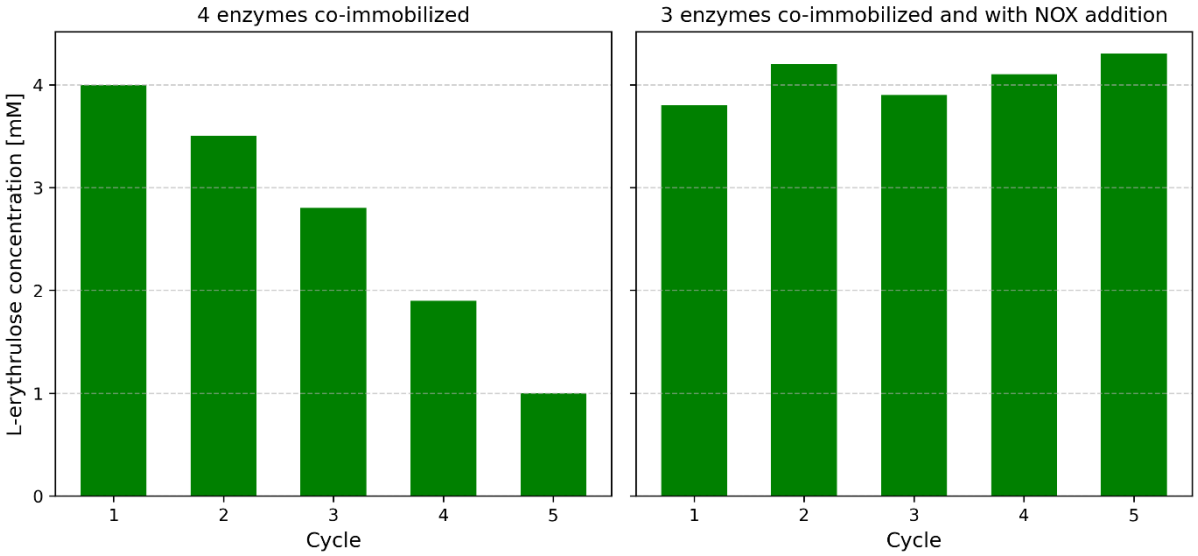

Figure 6: *L-erythrulose concentration measured over five reaction cycles after 1 hour: (left) co-immobilization of the four enzymes; (right) co-immobilization of three enzymes with fresh free NOX addition at each cycle. Reactions conditions: 25°C, 100 mM PPi pH 9, 50 mM glycerol, 50 mM formaldehyde, 0.5 mM NAD^+, 2 mg/mL GDH, 1.5 mg/mL NOX, 5 mg/mL FSA_{A129S} and 1 mg/mL catalase.*

Optimal conditions for maximizing L-erythrulose production were established by performing a fed-batch addition of both formaldehyde and immobilized NOX. To further increase productivity, the reaction was initiated with 150 mM glycerol, while maintaining the same immobilized enzymes loading and the same low NAD^+ concentration (0.5 mM). The initial formaldehyde concentration was 10 mM. Fresh additions of formaldehyde and NOX (immobilized separately on a fresh resin) were carried out at regular intervals during the

reaction (Figure 7). In this configuration, the enzyme inhibition by formaldehyde was minimized, and the deactivated NOX (see ESI, Section 14) was regularly replaced. Under these conditions, the reaction reached a yield of 80% after 108 hours, corresponding to a final concentration of 120 mM of L-erythrulose.

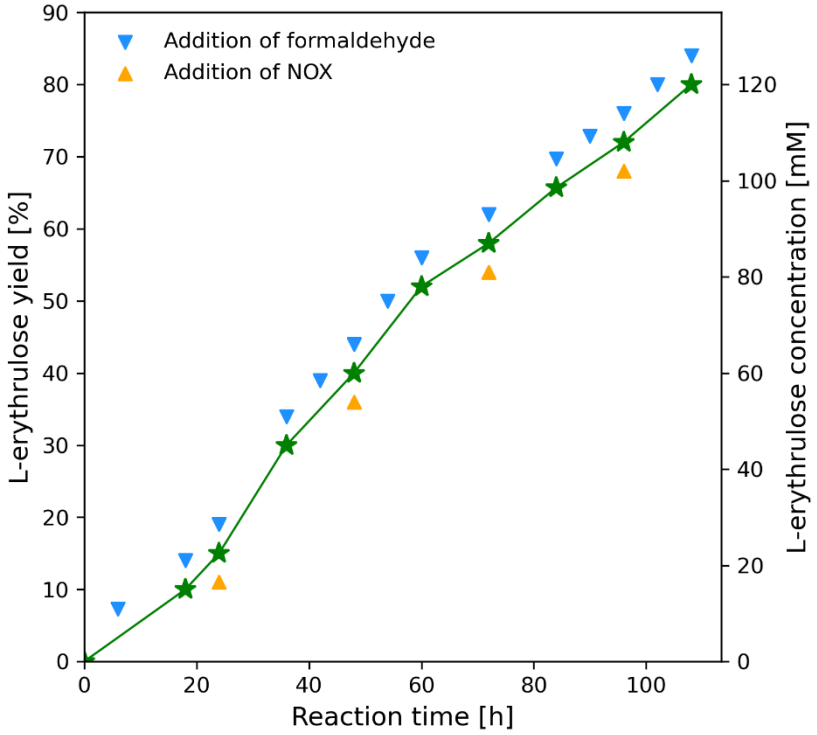

Figure 7: *Evolution of L-erythrulose yield and concentration as the function of reaction time by co-immobilized multi-enzyme cascade with multi additions of NOX and formaldehyde. Blue arrows illustrate the additions of formaldehyde (10 mM each) and the orange arrows illustrate the additions of 6 mg of immobilized NOX (medium concentration 1.5 mg/mL). Initial reactions conditions: 20°C, 100 mM PPi pH 9, 150 mM glycerol, 3 µL formaldehyde (10 mM), 0.5 mM NAD^+, 2 mg/mL GDH, 1.5 mg/mL NOX, 5 mg/mL FSA_{A129S} and 1 mg/mL catalase. Note: the experiment had to be stopped after 110h due to operational constraint, but the fact that no sign of deactivation was detected suggests the reaction can proceed to higher titers.*

An important aspect in the synthesis of rare sugars is the configuration of the desired product. In the case of aldolases [30,55,56], and FSA in particular, on the nucleophile side, there is no ambiguity regarding stereochemistry, since DHA is confined within the active site and can only present one of its faces (the generated enamine) to the aldehydic electrophile. To confirm that stereoselectivity is not altered by immobilization, a retro aldolisation assay of L-erythrulose and D-erythrulose was carried out (see ESI, Section 13). If the retroaldolisation reaction occurs,

DHA and formaldehyde are formed. Concentration of DHA can be measured by using GDH as auxiliary enzyme, reducing it to glycerol and monitoring the NADH consumption by UV-Vis spectrophotometry (340 nm). In the presence of L-erythrulose (Figure S10), NADH was consumed; in the presence of D-erythrulose, NADH concentration remained untouched (Figure S12), this confirms the strict specificity of immobilized FSA_{A129S}. Then, the same enzymatic assay was conducted on a reaction mixture collected after running the cascade reaction as described above (Figure S14). Here, the erythrulose formed via the cascade reaction was quantitatively retroaldolized by FSA_{A129S}, confirming that it was exclusively the L-isomer.

The cascade approach developed in this study, coupling glycerol oxidation and aldol condensation, solved instability or inhibition issues. Figure 8 illustrates the final L-erythrulose concentrations obtained from DHA or the final DHA concentrations obtained from glycerol (i.e. the two separate parts of the cascade) as reported in previous studies with various (bio)catalytic approaches. When comparing the results of this study with existing literature, it is evident that glycerol conversion is markedly increased. If the cascade reaction were conducted in two separate steps — first the blue box (DHA production), followed by the orange box (L-erythrulose yield) the overall yield would be lower. Here, the integration of both reactions in a one-pot concurrent system leads to substantially improved productivity. Furthermore, immobilization enhanced the productivity of the 4-enzymes cascade process. Finally, the addition of fresh immobilized NOX and formaldehyde in a fed-batch mode allowed to further boost the final L-erythrulose concentration.

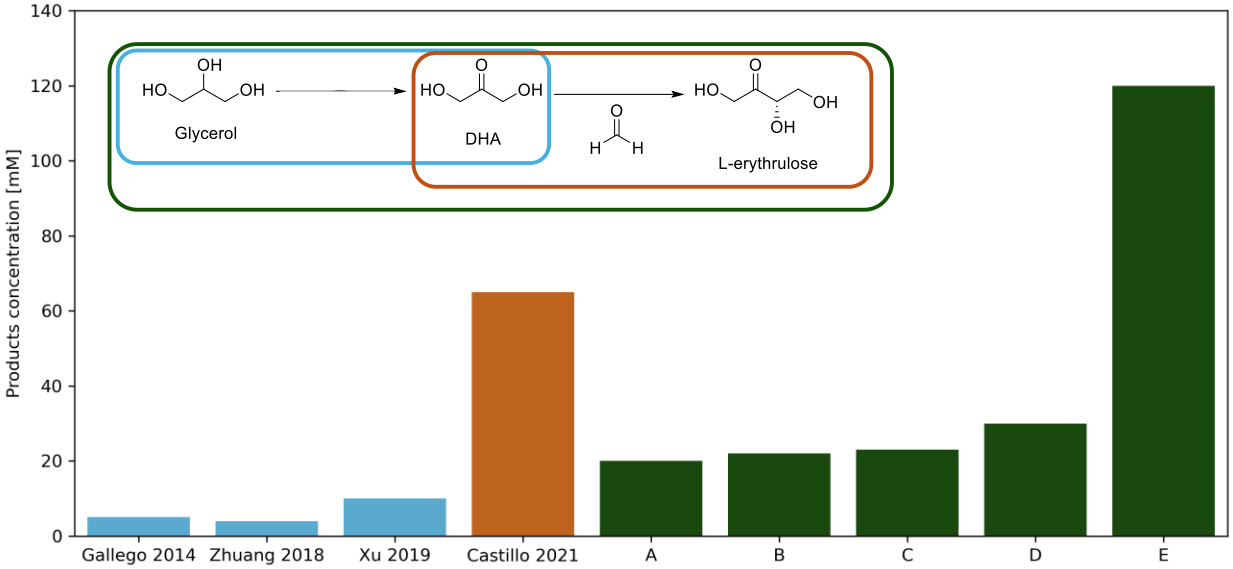

Figure 8: *Comparison of DHA production from glycerol (light blue), L-erythrulose production from DHA (orange) in the literature [21,25,25,31] and our work on the direct production of L-erythrulose from glycerol (green). A: free enzymes (Table 1, entry o). B: free enzymes with fed-batch additions of formaldehyde (see Figure 2). C: immobilized enzymes (see Figure 4). D: immobilized enzymes with fed-batch addition of formaldehyde (Figure 4). E: immobilized enzymes with fed-batch addition of fresh NOX and formaldehyde (see Figure 7).*

3. Conclusion

We developed a multi-enzymatic cascade based on four enzymes (GDH, NOX, FSA, and catalase) for the direct synthesis of rare sugar L-erythrulose from low-value glycerol. This upgrading scheme is more relevant than the one targeting DHA: the combination of FSA_{A129S} and NOX effectively prevented GDH inhibition by DHA and funneled the process towards the production of more valuable L-erythrulose with 100% selectivity. Cofactor recycling using NOX and H_2O_2 decomposition via catalase ensured that the reaction can be maintained even with a low input of NAD^+. In this 4-enzymes system, FSA_{A129S} and catalase exhibited high robustness; optimizing the tandem action of GDH and NOX was needed to boost productivity. The four-enzyme system was successfully co-immobilized on a commercial resin without enzyme leaching into the solution. However, NOX and formaldehyde were identified as the limiting factors: the former suffers from relatively rapid

turnover deactivation, and the second has a marked inhibition effect on several enzymes. This constrained the system to a L-erythrulose concentration of ~19 mM. To push the production further, a fed-batch reaction mode was proposed, involving the addition of fresh NOX and small aliquots of formaldehyde, leading to a sustained production of L-erythrulose; final concentration as high as 120 mM was demonstrated.

4. Bibliography

[1] Gérardy R, Debecker D P, Estager J, Luis P and Monbaliu J-C M 2020 Continuous Flow Upgrading of Selected C2–C6 Platform Chemicals Derived from Biomass *Chem. Rev.* **120** 7219–347

[2] Lari G M, Pastore G, Haus M, Ding Y, Papadokonstantakis S, Mondelli C and Pérez-Ramírez J 2018 Environmental and economical perspectives of a glycerol biorefinery *Energy Environ. Sci.* **11** 1012–29

[3] Bagnato G, Iulianelli A, Sanna A and Basile A 2017 Glycerol Production and Transformation: A Critical Review with Particular Emphasis on Glycerol Reforming Reaction for Producing Hydrogen in Conventional and Membrane Reactors *Membranes (Basel)* **7** 17

[4] Attarbachi T, Kingsley M and Spallina V 2024 Waste-derived low-grade glycerol purification and recovery from biorefineries: an experimental investigation *Biofuels, Bioproducts and Biorefining* **18** 1475–94

[5] Forrester M, Becker A, Hohmann A, Hernandez N, Lin F-Y, Bloome N, Johnson G, Dietrich H, Marcinko J, Chris Williams R and Cochran E 2020 RAFT thermoplastics from glycerol: a biopolymer for development of sustainable wood adhesives *Green Chemistry* **22** 6148–56

[6] Zhang H and Grinstaff M W 2014 Recent Advances in Glycerol Polymers: Chemistry and Biomedical Applications *Macromolecular Rapid Communications* **35** 1906–24

[7] Andreeva I V, Zaitsau D H, Qian S, Turovtzev V V, Pimerzin A A, Bara J E and Verevkin S P 2022 Glycerol valorisation towards biofuel additivities: Thermodynamic studies of glycerol ethers *Chemical Engineering Science* **247** 117032

[8] Soumoy L, Célis C, Debecker D P, Armandi M, Fiorilli S and Aprile C 2022 Hafnium-doped silica nanotubes for the upgrading of glycerol into solketal: Enhanced performances and in-depth structure-activity correlation *Journal of Catalysis* **411** 41–53

[9] Ramesh S and Debecker D P 2017 Room temperature synthesis of glycerol carbonate catalyzed by spray dried sodium aluminate microspheres *Catalysis Communications* **97** 102–5

[10] Ramesh S, Indukuri K, Riant O and Debecker D P 2018 Synthesis of Carbonate Esters by Carboxymethylation Using NaAlO2 as a Highly Active Heterogeneous Catalyst *Org. Process Res. Dev.* **22** 1846–51

[11] Karmee S K 2024 A review on preparation and applications of glycerol carbonate: Focus biocatalysis *Biocatalysis and Biotransformation* **42** 286–307

[12] Vivek N, Sindhu R, Madhavan A, Anju A J, Castro E, Faraco V, Pandey A and Binod P 2017 Recent advances in the production of value added chemicals and lipids utilizing biodiesel industry generated crude glycerol as a substrate – Metabolic aspects, challenges and possibilities: An overview *Bioresource Technology* **239** 507–17

[13] Matthijssen J, Rammal F, Scodeller I, Hickson M V, Van Vaerenbergh B, De Schrijver B, Carreira A S, Teixeira R F A, Debecker D P, Eloy P, Poleunis C, Makshina E V and Sels B F Amine-Catalyzed Aldol Addition of Dihydroxyacetone for Bio-Based Flame Retardants *ChemCatChem* **n/a** e01139

[14] Van der Verren M, Vykoukal V, Styskalik A, Malik A S, Aprile C and Debecker D P 2022 Airborne Preparation of Small Gold Nanoparticles Dispersed on Mesoporous Silica for the Catalytic Oxidation of Glycerol to Dihydroxyacetone *ACS Appl. Nano Mater.* **5** 18977–85

[15] Lee S, Kim H J, Lim E J, Kim Y, Noh Y, Huber G W and Kim W B 2016 Highly selective transformation of glycerol to dihydroxyacetone without using oxidants by a PtSb/C-catalyzed electrooxidation process *Green Chem.* **18** 2877–87

[16] Hirasawa S, Nakagawa Y and Tomishige K 2012 Selective oxidation of glycerol to dihydroxyacetone over a Pd–Ag catalyst *Catal. Sci. Technol.* **2** 1150–2

[17] Walgode P M, Faria R P V and Rodrigues A E 2021 A review of aerobic glycerol oxidation processes using heterogeneous catalysts: a sustainable pathway for the production of dihydroxyacetone *Catalysis Reviews* **63** 422–511

[18] Nishise H, Nagao A, Tani Y and Yamada H 1984 Further Characterization of Glycerol Dehydrogenase from Cellulomonas sp. NT3060 *Agricultural and Biological Chemistry* **48** 1603–9

[19] Wang X, Saba T, Yiu H H P, Howe R F, Anderson J A and Shi J 2017 Cofactor NAD(P)H Regeneration Inspired by Heterogeneous Pathways *Chem* **2** 621–54

[20] Minteer S, Tan B, Hickey D, Milton R and Giroud F 2015 Regeneration of the NADH Cofactor by a Rhodium Complex Immobilized on Multi-Walled Carbon Nanotubes *Journal of The Electrochemical Society* **162**

[21] Rocha-Martin J, Acosta A, Berenguer J, Guisan J M and Lopez-Gallego F 2014 Selective oxidation of glycerol to 1,3-dihydroxyacetone by covalently immobilized glycerol dehydrogenases with higher stability and lower product inhibition *Bioresour Technol* **170** 445–53

[22] Xu M-Q, Li F-L, Yu W-Q, Li R-F and Zhang Y-W 2020 Combined cross-linked enzyme aggregates of glycerol dehydrogenase and NADH oxidase for high efficiency in situ NAD+ regeneration *Int J Biol Macromol* **144** 1013–21

[23] Geueke B, Riebel B and Hummel W 2003 NADH oxidase from *Lactobacillus brevis*: a new catalyst for the regeneration of NAD *Enzyme and Microbial Technology* **32** 205–11

[24] Hummel W 1997 New alcohol dehydrogenases for the synthesis of chiral compounds *Adv Biochem Eng Biotechnol* **58** 145–84

[25] Zhuang M-Y, Jiang X-P, Ling X-M, Xu M-Q, Zhu Y-H and Zhang Y-W 2018 Immobilization of glycerol dehydrogenase and NADH oxidase for enzymatic synthesis of 1,3-dihydroxyacetone with in situ cofactor regeneration *Journal of Chemical Technology & Biotechnology* **93** 2351–8

[26] Garone M, Howard J and Fabrikant J 2015 A Review of Common Tanning Methods *J Clin Aesthet Dermatol* **8** 43–7

[27] Calderon-Ardila S, Matthijssen J, Van Huffel B, Péruch O, Morvan D, Bellière-Baca V, Dusselier M and Sels B F 2022 Establishing the Reaction Pathways of the Catalytic Conversion of Erythrulose to Sulphides of Alpha-Hydroxy Thioesters and Esters *ChemCatChem* **14** e202101730

[28] Murga J, Ruiz P, Falomir E, Carda M, Peris G and Marco J A 2004 Stereoselective Anti Aldol Reactions of Erythrulose Derivatives. Functionalized Chiral d3 and d4 Synthons *J. Org. Chem.* **69** 1987–92

[29] Marco J A, Carda M, González F, Rodríguez S, Castillo E and Murga J 1998 Diastereoselectivity in Organometallic Additions to the Carbonyl Group of Protected Erythrulose Derivatives *J. Org. Chem.* **63** 698–707

[30] Hélaine V, Gastaldi C, Lemaire M, Clapés P and Guérard-Hélaine C 2022 Recent Advances in the Substrate Selectivity of Aldolases *ACS Catal.* **12** 733–61

[31] Castillo J A, Guérard-Hélaine C, Gutiérrez M, Garrabou X, Sancelme M, Schürmann M, Inoue T, Hélaine V, Charmantray F, Gefflaut T, Hecquet L, Joglar J, Clapés P, Sprenger G A and Lemaire M 2010 A Mutant D-Fructose-6-Phosphate Aldolase (Ala129Ser) with Improved Affinity towards Dihydroxyacetone for the Synthesis of Polyhydroxylated Compounds *Advanced Synthesis & Catalysis* **352** 1039–46

[32] Babich L, Hemert L J C van, Bury A, Hartog A F, Falcicchio P, Oost J van der, Herk T van, Wever R and Rutjes F P J T 2011 Synthesis of non-natural carbohydrates from glycerol and aldehydes in a one-pot four-enzyme cascade reaction *Green Chem.* **13** 2895–900

[33] Yang J, Li J, Men Y, Zhu Y, Zhang Y, Sun Y and Ma Y 2015 Biosynthesis of l-Sorbose and l-Psicose Based on C-C Bond Formation Catalyzed by Aldolases in an Engineered Corynebacterium glutamicum Strain *Appl Environ Microbiol* **81** 4284–94

[34] Simon G, Eljezi T, Legeret B, Charmantray F, Castillo J A, Guérard-Hélaine C, Lemaire M, Bouzon M, Marlière P, Hélaine V and Hecquet L 2013 Synthesis of Specially Designed Probes to Broaden Transketolase Scope *ChemCatChem* **5** 784–95

[35] Li Z, Li F, Cai L, Chen Z, Qin L and Gao X-D 2020 One-Pot Multienzyme Synthesis of Rare Ketoses from Glycerol *J. Agric. Food Chem.* **68** 1347–53

[36] Gao Y, Chen Z, Nakanishi H and Li Z 2023 Highly Efficient Synthesis of Rare Sugars from Glycerol in Endotoxin-Free ClearColi by Fermentation *Foods* **12** 3078

[37] Romero E O, Saucedo A T, Hernández-Meléndez J R, Yang D, Chakrabarty S and Narayan A R H 2023 Enabling Broader Adoption of Biocatalysis in Organic Chemistry *JACS Au* **3** 2073–85

[38] Morokutti A, Lyskowski A, Sollner S, Pointner E, Fitzpatrick T B, Kratky C, Gruber K and Macheroux P 2005 Structure and function of YcnD from Bacillus subtilis, a flavin-containing oxidoreductase *Biochemistry* **44** 13724–33

[39] Bartoszek M and Sułkowski W W 2006 The Study of pH Influence on Bovine Liver Catalase by Means of UV-VIS Spectroscopyand Spin Labelling Method

[40] Tang C T, Ruch F E and Lin C C 1979 Purification and properties of a nicotinamide adenine dinucleotide-linked dehydrogenase that serves an Escherichia coli mutant for glycerol catabolism *J Bacteriol* **140** 182–7

[41] Zhu J, Chen P, Lu G, Liu P and Dong G 2019 Ruthenium-Catalyzed Reductive Cleavage of Unstrained Aryl–Aryl Bonds: Reaction Development and Mechanistic Study *J. Am. Chem. Soc.* **141** 18630–40

[42] Jankins T C, Berger B, Aouane F A, Barbeira-Arán S, Didier C, Hürlimann B, Zimmer C and Morandi B 2025 C–H Functionalization via Single Atom Metathesis of C–H and C–X Bonds *J. Am. Chem. Soc.* **147** 22314–21

[43] Gadona C, Royer L, Joly M, Hecquet L and Charmantray F 2025 Rare Ketose Synthesis from Glycolaldehyde by C2 Elongation of Aldoses Catalyzed by Transketolase Variants *ACS Catal.* **15** 7979–92

[44] Drozdz R and Naskalski J W 1993 Inactivation and denaturation of some proteins by enzyme system: myeloperoxidase, chloride and hydrogen peroxide *Folia Histochem Cytobiol* **31** 71–5

[45] Gastaldi C, Mekhloufi G, Forano C, Gautier A and Guérard-Hélaine C 2022 Mixing chemo- and biocatalysis for rare monosaccharide production by combining aldolase and N-heterocyclic carbene gold catalysts *Green Chem.* **24** 3634–9

[46] Guisan J M, Fernandez-Lorente G, Rocha-Martin J and Moreno-Gamero D 2022 Enzyme immobilization strategies for the design of robust and efficient biocatalysts *Current Opinion in Green and Sustainable Chemistry* **35** 100593

[47] Sheldon R A, Basso A and Brady D 2021 New frontiers in enzyme immobilisation: robust biocatalysts for a circular bio-based economy *Chem. Soc. Rev.* **50** 5850–62

[48] Arango H M, Biggelaar L van den, Soumillion P, Luis P, Leyssens T, Paradisi F and Debecker D P 2023 Continuous flow-mode synthesis of (chiral) amines with transaminase: a strategic biocatalytic approach to essential building blocks *React. Chem. Eng.* **8** 1505–44

[49] Bu Y, Zhang T, Jiang B and Chen J 2021 Improved Performance of D-Psicose 3-Epimerase by Immobilisation on Amino-Epoxide Support with Intense Multipoint Attachment *Foods* **10** 831

[50] Perçin Z, Kursula L, Löfgren E, Byström E, Kexel F, Bubenheim P, Schlüter M and Liese A 2024 Intensification of a biocatalytic oxidation under fine bubble aeration in a rotating bed reactor *Biochemical Engineering Journal* **207** 109333

[51] Franceus J and Desmet T 2020 Sucrose Phosphorylase and Related Enzymes in Glycoside Hydrolase Family 13: Discovery, Application and Engineering *Int J Mol Sci* **21** 2526

[52] Muley A B, Chaudhari S A, Bankar S B and Singhal R S 2019 Stabilization of cutinase by covalent attachment on magnetic nanoparticles and improvement of its catalytic activity by ultrasonication *Ultrasonics Sonochemistry* **55** 174–85

[53] Dias Gomes M, Bommarius B R, Anderson S R, Feske B D, Woodley J M and Bommarius A S 2019 Bubble Column Enables Higher Reaction Rate for Deracemization of (R,S)-1-Phenylethanol with Coupled Alcohol Dehydrogenase/NADH Oxidase System *Advanced Synthesis & Catalysis* **361** 2574–81

[54] Al-Shameri A, Siebert D L, Sutiono S, Lauterbach L and Sieber V 2023 Hydrogenase-based oxidative biocatalysis without oxygen *Nat Commun* **14** 2693

[55] Fessner W-D and Helaine V 2001 Biocatalytic synthesis of hydroxylated natural products using aldolases and related enzymes *Current Opinion in Biotechnology* **12** 574–86

[56] Clapés P and Garrabou X 2011 Current Trends in Asymmetric Synthesis with Aldolases *Advanced Synthesis & Catalysis* **353** 2263–83